

Figure 4 Mineral nitrogen ($\text{NO}_3^- + \text{NH}_4^+$) concentrations for C horizon soils. These soils have phyllite parent rock in Jack Creek watershed. Top panel, data for *in situ* soil solutions extracted from soil samples via centrifugation¹⁷, bottom panel, KCl-extractable nitrogen¹⁸ from the same soil samples ($n = 3$). Data from the 1995–96 and 1996–97 water years show a similar pattern of high total mineral N at the beginning of the water year, and lower concentrations following progressive leaching of the soil profile.

much of California's surface water supply. Given the widespread occurrence of sedimentary and metasedimentary rocks on the Earth's surface^{7,23–31} and the large inventory of nitrogen contained within these rocks⁸, the role of geological nitrogen as a non-point source of nitrate contamination in surface waters needs to be re-evaluated. □

Received 7 July 1997; accepted 28 July 1998

1. Galloway, J. N., Schlesinger, W. H., Levy, H., Michaels, A. & Schnoor, J. L. Nitrogen fixation: anthropogenic enhancement—environmental response. *Glob. Biogeochem. Cycles* **9**, 235–252 (1995).
2. Power, J. F. & Papendick, R. I. in *Fertilizer Technology and Use* (ed. Engelstad, O. P.) 503–520 (Soil Sci. Soc. Am., Madison, Wisconsin, 1985).
3. Spalding, R. F. & Exner, M. E. Occurrence of nitrate in groundwater—a review. *J. Environ. Qual.* **22**, 393–402 (1993).
4. Keeney, D. R. in *CRC Critical Reviews in Environmental Control* (ed. Straub, C. P.) 257–304 (CRC, Boca Raton, Florida, 1986).
5. Likens, G. E., Bormann, F. H., Johnson, N. M., Fisher, D. W. & Pierce, R. S. Effects of forest cutting and herbicide treatment on nutrient budgets in the Hubbard Brook watershed-ecosystem. *Ecol. Monogr.* **40**, 23–47 (1970).
6. Bouchard, D. C., Williams, M. K. & Surampalli, R. Y. Nitrate contamination of groundwater: sources and potential health effects. *J. Am. Wat. Works Assoc.* **84**, 85–90 (1992).
7. Blatt, H. & Jones, R. L. Proportions of exposed igneous, metamorphic, and sedimentary rocks. *Geol. Soc. Am. Bull.* **86**, 1085–1088 (1975).
8. Schlesinger, W. H. *Biogeochemistry—An Analysis of Global Change* (Academic, San Diego, California, 1997).
9. Goldman, C. R. Primary productivity, nutrients, and transparency during the early onset of eutrophication in ultra-oligotrophic Lake Tahoe, California–Nevada. *Limnol. Oceanogr.* **33**, 1321–1333 (1988).
10. Wagner, D. L., Jennings, C. W., Bedrossian, T. L. & Bortugno, E. J. *Geologic Map of the Sacramento Quadrangle, California* (Calif. Div. Geology, Sacramento, California, 1981).
11. Clark, L. D. Stratigraphy and structure of part of the western Sierra Nevada metamorphic belt, California. *Prof. Pap. US Geol. Surv.* **410**, (1964).
12. Duffield, W. A. & Sharp, R. V. Geology of the Sierra Foothills melange and adjacent areas, Amador County, California. *Prof. Pap. US Geol. Surv.* **827**, (1975).
13. Schroeder, P. A. & Ingall, E. D. A method for the determination of nitrogen in clays, with application to the burial diagenesis of shales. *J. Sedim. Res.* **64**, 694–697 (1994).
14. Douglas, L. A. in *Minerals in Soil Environments* 2nd edn (eds Dixon, J. B. & Weed, S. B.) 635–674 (Soil Sci. Soc. Am., Madison, Wisconsin, 1989).
15. Kulandaiswamy, V. C. & Seetharaman, S. A note on Barnes' method of hydrograph separation. *J. Hydrol.* **9**, 222–229 (1969).
16. Caisie, D., Pollock, T. L. & Conjak, R. A. Variation in stream water chemistry and hydrograph separation in a small drainage basin. *J. Hydrol.* **178**, 137–157 (1996).
17. Dahlgren, R. A. Comparison of soil solution extraction procedures: effect on solute chemistry. *Commun. Soil Sci. Plant Anal.* **24**, 1783–1794 (1993).
18. Bundy, L. G. & Meisinger, J. J. in *Methods of Soil Analysis Part 2, Microbiological and Biochemical Properties* 2nd edn (eds Page, A. L., Miller, R. H. & Kenney, D. R.) 951–984 (Soil Sci. Soc. Am., Madison, Wisconsin, 1982).
19. Parfitt, R. L., Percival, H., Dahlgren, R. A. & Hill, L. F. Soil and soil solution chemistry under pasture and radiata pine in New Zealand. *Plant Soil* **191**, 279–290 (1997).
20. Aber, J. D., Nadelhoffer, K. J., Steudler, P. & Melillo, J. M. Nitrogen saturation in northern forest ecosystems. *BioScience* **39**, 378–386 (1989).
21. Dahlgren, R. A., Singer, M. J. & Huang, X. Oak tree and grazing impacts on soil properties and nutrients in a California oak woodland. *Biogeochemistry* **39**, 45–64 (1997).
22. Pavlik, B. M., Muick, P. C., Johnson, S. & Popper, M. *Oaks of California* (Cachuma, Los Olivos, California, 1991).

23. Boyd, S. R., Hall, A. & Pillinger, C. T. The measurement of delta ¹⁵N in crustal rocks by static vacuum mass spectrometry: application to the origin of the ammonium in the Cornubian batholith, southwest England. *Geochim. Cosmochim. Acta* **57**, 1339–1347 (1993).
24. Duit, W., Jansen, J. B. H., van Breemen, A. & Bos, A. Ammonium micas in metamorphic rocks as exemplified by Dome de l'Agout (France). *Am. J. Sci.* **286**, 702–732 (1986).
25. Eugster, H. P. & Munoz, J. Ammonium micas: possible sources of atmospheric ammonia and nitrogen. *Science* **151**, 683–686 (1965).
26. Hall, A., Pereira, M. D. & Bea, F. The abundance of ammonium in the granites of central Spain, and the behaviour of the ammonium ion during anatexis and fractional crystallization. *Mineral. Petrol.* **56**, 105–123 (1996).
27. Kawano, M. & Tomita, K. Mineralogical properties of interstratified ammonium-bearing mica/smectites from Aira, Kagoshima Prefecture, Japan. *Mineral. J.* **15**, 19–31 (1990).
28. Krohn, M. D., Kendall, C., Evans, J. R. & Fries, T. L. Relations of ammonium minerals at several hydrothermal systems in the western U.S. *J. Volcanol. Geotherm. Res.* **56**, 401–413 (1993).
29. Meyer, F. M. & Ridgway, J. Ammonium in Witwatersrand reefs: a possible indicator of metamorphic fluid flow. *S. Afr. J. Geol.* **1994**, 343–347 (1991).
30. Ridgway, J., Appleton, J. D. & Levinson, A. A. Ammonium geochemistry in mineral exploration—comparison of results from the American cordilleras and the southwest Pacific. *Appl. Geochem.* **5**, 475–489 (1990).
31. Stevenson, F. J. Chemical state of the nitrogen in rocks. *Geochim. Cosmochim. Acta* **26**, 797–809 (1962).
32. SYSTAT v. 6.0 for Windows (SPSS Inc., Chicago, Illinois, 1996).

Acknowledgements. We thank Georgia Pacific for helicopter access to high-elevation watersheds during the winter; East Bay Municipal Utilities District, Georgia Pacific, and the US Forest Service for the loan of streamwater autosamplers; J. Munn, B. McGurk, L. Costock, J. Pierner, B. Smith and the Mokelumne River Water Quality Monitoring Committee for logistical support; and J. Jimenez, D. Levine, R. Northup, G. Pauly, J. Shaw, E. Suzuki and D. Walsh for assistance with field work and analysis. This work was supported by the California Dept of Forestry and Fire Protection.

Correspondence and requests for materials should be addressed to R.A.D. (e-mail: radahlgren@ucdavis.edu).

Cenozoic magmatism throughout east Africa resulting from impact of a single plume

C. J. Ebinger*† & N. H. Sleep*

* Department of Geophysics, Mitchell Building, Stanford University, Stanford, California 94305, USA

† Department of Earth Sciences, University of Leeds, Leeds LS2 9JT, UK

The geology of northern and central Africa is characterized by broad plateaux, narrower swells and volcanism occurring from ~45 Myr ago to the present. The greatest magma volumes occur on the >1,000-km-wide Ethiopian and east African plateaux, which are transected by the Red Sea, Gulf of Aden and east African rift systems, active since the late Oligocene epoch. Evidence for one or more mantle plumes having impinged beneath the plateaux comes from the dynamic compensation inferred from gravity studies, the generally small degrees of extension observed and the geochemistry of voluminous eruptive products^{1–4}. Here we present a model of a single large plume impinging beneath the Ethiopian plateau that takes into account lateral flow and ponding of plume material in pre-existing zones of lithospheric thinning⁵. We show that this single plume can explain the distribution and timing of magmatism and uplift throughout east Africa. The thin lithosphere beneath the Mesozoic–Palaeogene rifts and passive margins of Africa and Arabia guides the lateral flow of plume material west to the Cameroon volcanic line and south to the Comoros Islands. Our results demonstrate the strong control that the lithosphere exerts on the spatial distribution of plume-related melting and magmatism.

The alkali volcanism without rifting on the ~400-km-wide topographic swells and ocean island chains of Africa (Fig. 1) have been attributed to separate plumes^{1,6,7}. Burke¹ suggested that the unusually high elevation and Cenozoic volcanism stems from the African plate's standstill relative to mantle circulation since ~35 Myr ago, which allowed ~40 mantle plumes to penetrate the plate without the creation of hotspot tracks. The Hoggar, Tibesti, Darfur and Adamawa swells and Cenozoic eruptive centres lie near

Mesozoic rifts, and a Mesozoic–Palaeogene rift system underlies the topographic depression between the east African and Ethiopian plateaux^{6,8} (Fig. 1). Wilson and Guiraud⁶ have suggested preferential melting of mantle metasomatized during the Mesozoic breakup of Gondwana, in the presence of many plumes.

Seismic velocity and geochemical anomalies suggest that hot upper mantle underlies the Red Sea, Afar and Eastern rifts^{9–11}. Tomographic models show >200-km-thick lithosphere beneath the cratonic core of east Africa and steep gradients along its margins¹¹, but little is known of upper-mantle structure beneath the Ethiopian plateau away from the rifts (Fig. 1). Marty *et al.*² have reported high ³He/⁴He ratios throughout a 2,000-km-wide region centred on the Ethiopian plateau, indicating a broad mantle thermal anomaly. The largest geoid anomalies coincide with the Ethiopian and east African plateaux where more than $8 \times 10^5 \text{ km}^3$ of primarily basaltic material has erupted^{3,12} since ~45 Myr ago. The earliest Cenozoic flood basaltic magmatism occurred in the Ethiopian plateau region, although the Cameroon chain onshore has seen discontinuous activity since Late Cretaceous time^{1,13} (Fig. 1).

Incomplete thermal equilibration of thinned lithosphere beneath Late Cretaceous–Palaeogene rifts and Mesozoic passive margins would have caused significant variations in the depth to the 1,300 °C isotherm (base of lithosphere) beneath Africa 45 Myr ago, particu-

larly in basins active during Palaeogene time (Fig. 1). This topographic relief at the lithosphere–asthenosphere boundary before the arrival of a plume head may have deflected plume material away from its centre, as would cratonic roots. In the numerical models of Sleep^{5,14}, topographic relief at the lithosphere–asthenosphere boundary disrupts the radial spread of buoyant plume material, leading to ponding below thinner lithosphere. Melting is enhanced where plume material cascades over steep relief at the lithosphere–asthenosphere boundary⁵.

The question is, could melt generated from the impact of one strong plume beneath the Ethiopian plateau flow along the elevated lithosphere–asthenosphere boundary beneath the Mesozoic–Palaeogene rifts and passive margins, explaining the swells with small volumes of erupted magma shown in Fig. 1. We use the methods of Sleep⁵ to investigate the effects of pre-existing lithospheric thickness variations on the lateral flow of plume material. Our predictions of the spatial distribution of plume material have implications for the reactivation of pre-plume rifts and the preservation of cratonic roots.

Below and in Figs 1 and 2a we summarize constraints on lithospheric structure before and after initial magmatism in the Ethiopian plateau region. Mantle xenolith and seismic data indicate that Archaean–early Proterozoic lithosphere was >150 km thick

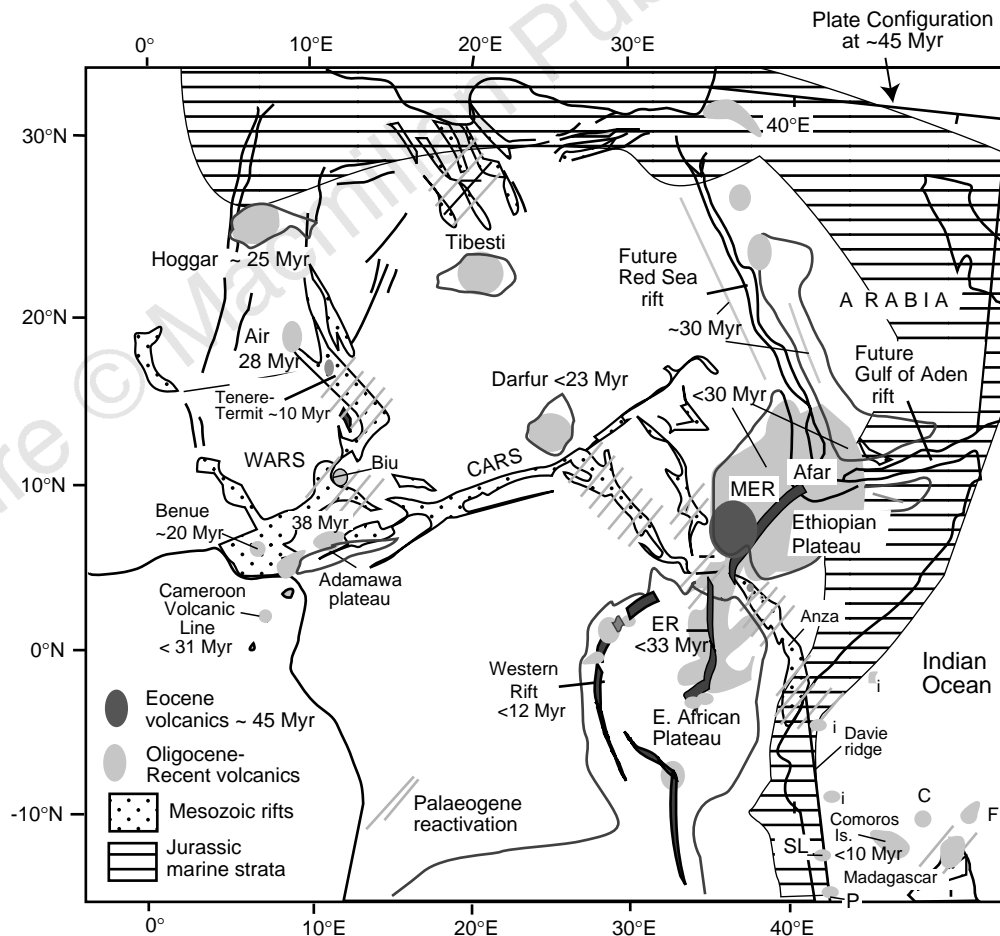


Figure 1 Reconstruction of the African plate at ~45 Myr ago, before the separation of Africa and Arabia. Shown are Cenozoic plateaux, swells, rifts (ER, Eastern rift; MER, Main Ethiopian rift) and magmatism (maximum ages in each province indicated), the distribution of Mesozoic–Palaeogene rifts, and marine strata along passive margins (after ref. 18). Elevations >1,000 m are enclosed by bold lines; uplift (where known) occurred after ~32 Myr ago (ref. 17). Where known from borehole data, peak extension in pre-plume basins occurred in Cretaceous time^{8,16,18,34}. Seismic reflection and borehole data indicate renewed extension during Eocene–recent time in the west African (WARS), central African (CARS)

and Anza rift systems^{8,16,17,31,34}. Lithospheric extension along the Indian Ocean passive margin occurred in Jurassic time; sea-floor spreading between Africa and Madagascar occurred between 165 and 80 Myr ago (ref. 35). Volcanism and extension have also affected the passive margins of east Africa since ~35 Myr ago with reactivation of some Mesozoic structures³⁵ (for example, Davie ridge). Volcanoes of the Comoros chain have developed on oceanic crust since 5 Myr ago, and the Cosmoledo (C), Farquhar (F), St Lazaire (SL) and Paisley (P) seamounts are of similar age^{7,35}; i indicates intrusives.

beneath parts of central and northern Africa 45 Myr ago (refs 11, 15). We assume that cratonic lithosphere was ~150 km thick; thicker lithosphere would only enhance the lateral flow effects we describe below. We use extension estimates, where available, to constrain lithospheric thickness beneath the Mesozoic–Palaeogene rifts and passive margins, assuming uniform crust and upper-mantle extension (Fig. 2a). Sequences within many of these basins show a thermal subsidence phase, indicating that the mantle lithosphere was thinned^{18,16–18}.

Volcanism in southwestern Ethiopia 40–45 Myr ago occurred ~20 Myr before the earliest known extension in this area^{12,19} (Fig. 1). Between ~32 and 25 Myr ago, volcanism was widespread throughout the Red Sea and Gulf of Aden, northern Main Ethiopian rift (MER), and central Ethiopian plateau^{17,19–22} (Fig. 1). The geochemical signature of the plume now extends into the Red Sea and Gulf of Aden^{2,23}, and seismic data suggest crustal underplating beneath the 2,500-m-high eastern plateau⁹.

Far-field stresses generated by the Africa–Eurasia collision may have initiated extension in parts of the Red Sea and Gulf of Aden rifts ~30 Myr ago^{17,20}. Sea-floor spreading commenced ~20 Myr ago in the Gulf of Aden, propagating westward into Afar by ~5 Myr ago (ref. 17). Alkaline volcanism and faulting have propagated southward along the Eastern and Western rifts since 25 Myr ago (Fig. 1). Where timing constraints exist, extension within any province, if present, occurs after initial uplift and volcanism, except in the pre-plume rift zones and along passive margins^{17,19–22}. Overall, we see a sub-radial distribution of magmatism about southwestern Ethiopia since ~45 Myr ago.

Hot, low-density material within starting mantle plumes rises diapirically through the mantle and interacts with the base of the lithosphere, forming a broad head that may partially melt to produce flood basalts and radial dykes^{24,25}. This buoyant material displaces denser, normal asthenosphere and heats the lithosphere,

leading to regional uplift, lithospheric thinning and pressure-release magmatism. General models differ in the interactions between plume and lithosphere and the timing of pressure-release volcanism, with variations in plume temperatures of ~10 K leading to significant variations in melt volumes^{26,27}. Sleep^{5,14} shows that pre-existing zones of lithospheric thinning act as sinks for buoyant plume material, driving lateral flow hundreds of kilometres from the plume's centre.

Using the analytical and numerical methods of Sleep^{5,14}, we delineate areas of ponded plume material that are prone to pressure-release magmatism. Assuming a linear depth versus melting parametrization²⁸, we can predict final melt thickness above the plume. We do not distinguish between plume head and tail material, given the slow movement of the African plate since 45 Myr ago. We assume that the plume initially was centred at 38° E, 8° N where the earliest basalts are found, and that it moves to 36° E, 4° N over 45 Myr. Very similar results are obtained if the head is moved a few degrees in any direction.

The numerical model predicts the distribution of plume material and melt beneath central and northern Africa after onset (Fig. 2b, c). At ~45 Myr ago a circular plume head of 750 km radius impinges on the base of the lithosphere, producing a thick, low-density layer beneath the Ethiopian plateau. There is a net upward movement of laterally flowing plume material, with steep gradients increasing vertical velocity and pressure-release melting^{5,26} (Fig. 2c). Considering the thick lithospheric lid, local factors (for example, pre-existing weaknesses and volatile content) probably control eruptive centre locations.

By 40 Myr ago, plume material has moved an additional 500–800 km southward and eastward to thinned lithosphere along the Indian Ocean margin and beneath the Arabian peninsula, following Mesozoic–Palaeogene rifts. Between 35 and 10 Myr ago a narrow tongue of plume material ‘trickles’ westward beneath the central

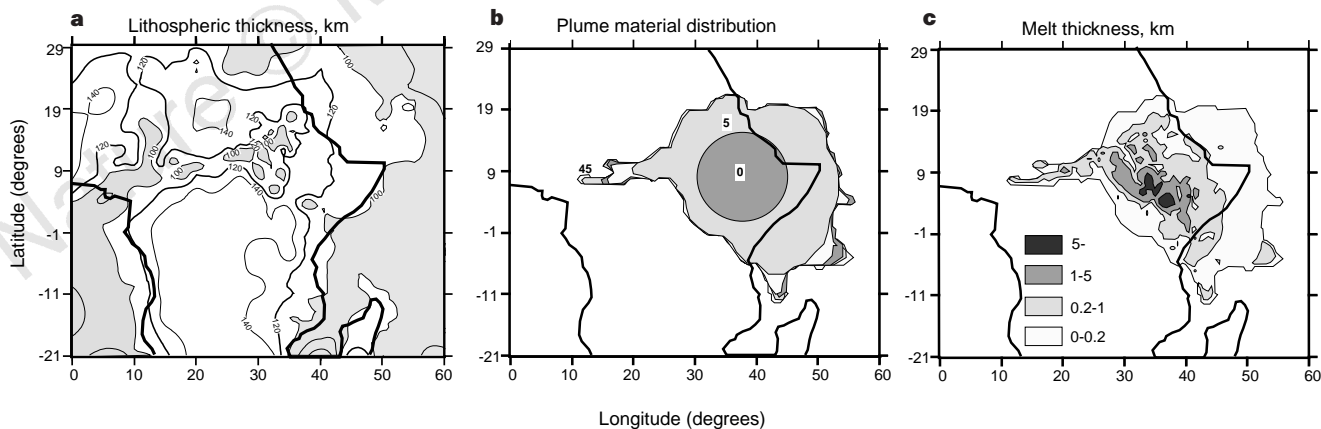


Figure 2 Results of plume model. **a**, Model of pre-plume lithospheric thickness (values <100 km are shaded) at ~45 Myr ago constrained by estimates of crustal stretching, seismic^{9–11,32} and xenolith^{15,30} data. Maximum crustal extension in Mesozoic–Palaeogene rift basins of the west and central African rift systems varies from <10% to ~50%, based on subsidence patterns, fault reconstructions, and models of gravity data^{8,16–18,34,35}. The northern and northeastern margins of Africa and much of the Arabian peninsula were passive margins into Palaeogene time; we assume 110–100-km-thick lithosphere here. Africa's northeastern margin was affected by folding in Late Cretaceous and Eocene time with the collision of Africa and Eurasia¹; we assume a ~115-km-thick lithosphere here. Oceanic lithosphere along Africa's eastern and western margins is assumed to follow a normal thermal subsidence curve until the onset of the plume at ~45 Myr ago, with formation ages assigned from the model of Coffin and Rabinowitz²⁵. **b**, Contours of the maximum horizontal extent of plume material between 45 Myr ago (contour 0) and present (contour 45) predicted by the interactions of plume

with the lithospheric lid shown in **a**. We note the lobe of plume material which roughly coincides with the Indian Ocean seamounts and intrusives, and the tongue of material beneath the central African rift system (Fig. 1). We use the same model parameters as Sleep¹⁴, except that we assume a starting plume head volume of $0.2 \times 10^{18} \text{ m}^3$, a viscosity of $0.3 \times 10^{18} \text{ Pa s}$ and a constant buoyancy flux of 4 Mg s^{-1} similar to that of a strong plume²⁷. Only local buoyancy is considered. As shown in Sleep¹⁴, the depth to the base or viscosity of the ordinary asthenospheric channel and its replenishment mechanism have little effect on results. This model reproduces the spreading drop similarity solution³⁶ to 0.5% at 45 Myr. **c**, The equivalent thickness of melt produced from 30 Myr ago to the present. The calculation includes pressure-release melting from lateral flow of material and lithospheric thinning caused by the interaction of plume material and the base of the lithosphere. Plume material is assumed to melt by 0.1% per kilometre of ascent, independent of depth. Melting is enhanced above steep gradients shown in **a**.

African rift zone, reaching the western Adamawa plateau by ~5 Myr ago. Our predictions for this region are probably minima due to the earlier history of plume activity and rifting in this area.

This simple model of lithosphere-plume interactions in Africa correlates well with the distribution and timing of magmatism in east and central Africa, and along the Indian Ocean margin (Figs 1, 2). For example, ponding and melting occur beneath the Darfur swell by 30 Myr ago, and beneath the Davie ridge by 5 Myr ago, explaining the young seamounts along this Mesozoic structure (Figs 1, 2). The radial flow of plume material away from the plume's centre fits well with the observed southward propagation of volcanism in east Africa since Late Oligocene time (Fig. 1). The Ethiopian plume model cannot explain the Tibesti or Hoggar swells, unless undiscovered rifts lie beneath the Sahara. We could increase the plume volume, lower viscosity, and modify initial lithospheric thickness to increase the radial flow, but too little information on present and ancient lithospheric structure exists to justify refinements of our simple model.

Our model includes only thermal thinning of the lithosphere above the plume material, but we can readily anticipate the model's response to lithospheric stretching within the Red Sea and Gulf of Aden. Newly thinned lithosphere would have channelled melt from the eastern limbs into the axis of the Red Sea and Aden rifts, as well as adjacent margins. This extension along the Arabian margins at ≤ 30 Myr ago would have triggered decompression melting of ponded plume material, causing widespread magmatism along the Arabian margins. The superposition of Red Sea, Aden and east African extension in Afar may have caused greater pressure-release melting there rather than above our plume's centre.

In active rifting models, lateral density variations within the upper mantle generate extensional stresses large enough to initiate rifting²⁹. Adiabatic decompression melting beneath the rift enhances flow of plume material, and rifts propagate. This mechanism may explain the extension after magmatism and uplift, and the southward propagation of rifting in east Africa. Although it is an indirect result, we suggest that episodic extension in the Red Sea and Gulf of Aden captured ponded melt, and led to pulses of basaltic magmatism in east Africa. Reactivation of pre-plume basins and initial extension in the northern Kenya rift ~25 Myr ago would have created a conduit for the distribution of plume material southward beneath the Eastern and Western rift systems (Figs 1, 2a). This additional extension not included in the model would increase outward flow, perhaps as far south as Madagascar and the Western rift where magmatic centres are located near Mesozoic rifts (Fig. 1).

The steep gradients at the lithosphere-asthenosphere boundary along the Tanzania craton/mobile-belt boundaries¹¹ may focus flow, explaining <30-Myr-old carbonatitic and kimberlitic magmas derived from small melt volumes at depths ≥ 150 km (refs 15, 30). The pre-plume relief at the lithosphere-asthenosphere boundary beneath the east African cratons diverts plume material and focuses decompression melting along the craton margins, preserving their thick, strong cores (Fig. 2c).

These results have implications for the rejuvenation and thermal subsidence of continental rifts. Ponded plume material contributes to regional uplift, but sills intruded into sedimentary strata or magma underplated at the base of previously thinned crust can locally augment or counter this uplift, depending on density contrasts. Many Mesozoic-Palaeogene rift basins lying along the predicted paths of plume material show Late Cenozoic reactivation and igneous intrusions^{16,31}, but borehole and seismic data are available from many basins. Coffin *et al.*³² report anomalous upper-mantle velocities of 7.8 km s^{-1} beneath the western Indian Ocean basin, suggesting that mantle temperatures are elevated above the southeastern lobe (Fig. 2c).

Melt composition will vary depending on plume interactions with the heated lithosphere and normal asthenosphere, which will increase with distance from the source. Temporal variations will

occur due to compositional and temperature differences between plume head and tail³³.

Our studies demonstrate that the location of continental flood basalts may not coincide with the centre of the starting plume head, and several discrete magmatic provinces can be produced by a single plume. This numerical model of the Ethiopian plume also supports a plume origin for the east African rift system. □

Received 28 July 1997; accepted 6 August 1998.

- Burke, K. The African plate. *S. Afr. J. Geol.* **99**, 339–410 (1996).
- Marty, B., Pik, R. & Gezahagen, Y. He isotopic variations in Ethiopian plume lavas: nature of magmatic sources and limit on lower mantle convection. *Earth Planet. Sci. Lett.* **144**, 223–237 (1996).
- Latin, D., Norry, M. & Tarzey, R. Magmatism in the Gregory rift: evidence for melt generation by a plume. *J. Petrol.* **34**, 1007–1027 (1993).
- Ebinger, C., Bechtel, T., Forsyth, D. & Bowin, C. Effective elastic plate thickness beneath the East African and Afar plateaux, and isostatic compensation for the uplifts. *J. Geophys. Res.* **94**, 2893–2901 (1989).
- Sleep, N. H. Lateral flow of hot plume material ponded at sub-lithospheric depths. *J. Geophys. Res.* **101**, 28065–28083 (1996).
- Wilson, M. & Giraud, R. Magmatism and rifting in western and central Africa, from Late Jurassic to recent times. *Tectonophysics* **213**, 203–225 (1993).
- Emerick, C. M. & Duncan, R. Age progressive volcanism in the Comores Archipelago, western Indian Ocean and implications for Somali plate motion. *Earth Planet. Sci. Lett.* **60**, 415–428 (1982).
- Hendrie, D., Kuszniir, N., Morley, C. K. & Ebinger, C. A quantitative model of rift basin development in the northern Kenya rift: evidence for the Turkana region as an "accommodation zone" during the Palaeogene. *Tectonophysics* **236** 409–438 (1994).
- Prodehl, C. & Mechie, J. Crustal thinning in relationship to the evolution of the Afro-Arabian rift system: A review of seismic refraction data. *Tectonophysics* **198**, 311–327 (1991).
- Green, V., Achauer, U. & Meyer, R. A three-dimensional image of the crust and upper mantle beneath the Kenya rift. *Nature* **354**, 199–203 (1991).
- Ritsma, J., Nyblade, A., Owens, T., Langston, C. & VanDecar, J. Upper mantle velocity structure beneath Tanzania, E. Africa: implications for the stability of cratonic lithosphere. *J. Geophys. Res.* (in the press).
- George, R. *Thermal and Tectonic Controls on Magmatism in the Ethiopian Rift*. Thesis, Open Univ. (1997).
- Lee, D. C., Halliday, A. N., Fitton, J. G. & Pol, G. Chronology of volcanism along the Cameroon volcanic line. *Earth Planet. Sci. Lett.* **123**, 119–138 (1994).
- Sleep, N. Lateral flow and ponding of starting plume material. *J. Geophys. Res.* **102**, 10001–10012 (1997).
- Boyd, F. & Gurney, J. Diamonds in the African lithosphere. *Science* **232**, 272–477 (1986).
- Genik, G. Regional framework, structure, and petroleum aspects of rift basins in Niger, Chad, and Central African Republic. *Tectonophysics* **213**, 169–185 (1992).
- Menzies, M., Gallagher, K., Yelland, A. & Hurford, A. Volcanic and nonvolcanic rifted margins of the Red Sea and Gulf of Aden: crustal cooling and margin evolution in Yemen. *Geochim. Cosmochim. Acta* **61**, 2511–2527 (1997).
- Bosworth, W. Mesozoic and Tertiary rifting in East Africa. *Tectonophysics* **209**, 115–137 (1992).
- Ebinger, C. J., Yemane, T., WoldeGabriel, G. & Aronson, J. Late Eocene-Recent volcanism and faulting in the southern Main Ethiopian rift system. *J. Geol. Soc. Lond.* **150**, 99–108 (1993).
- Baker, J., Snee, L. & Menzies, M. A brief Oligocene period of flood volcanism in Yemen: implications for the duration and rate of continental flood volcanism at the Afro-Arabian triple junction. *Earth Planet. Sci. Lett.* **138**, 39–55 (1996).
- Morley, C. K. *et al.* Tectonic evolution of the northern Kenya rift. *J. Geol. Soc. Lond.* **149**, 333–348 (1992).
- Hofmann, C. Timing of the Ethiopian flood basalt event and implications for plume birth and global change. *Nature* **389**, 838–841 (1997).
- Schilling, J.-G., Kingsley, R., Hanan, B. & McCully, B. Nd-Sr-Pb isotopic variations along the Gulf of Aden: evidence for the Afar mantle plume-lithosphere interaction. *J. Geophys. Res.* **97**, 10927–10966 (1992).
- Griffiths, R. & Campbell, I. Interaction of mantle plume heads with Earth's surface at the onset of small-scale convection. *J. Geophys. Res.* **96**, 18295–18310 (1991).
- Hill, R. I. Starting plumes and continental break-up. *Earth Planet. Sci. Lett.* **104**, 398–416 (1991).
- White, R. & McKenzie, D. Magmatism at rift zones: the generation of volcanic continental margins and flood basalts. *J. Geophys. Res.* **94**, 7685–7729 (1989).
- Ribe, N. & Christensen, U. Three-dimensional modeling of plume-lithosphere interaction. *J. Geophys. Res.* **99**, 669–682 (1994).
- Watson, S. & McKenzie, D. Melt generation by plumes: a study of Hawaiian volcanism. *J. Petrol.* **32**, 501–537 (1991).
- Crough, S. T. Thermal origin of midplate swells. *Geophys. J. R. Astron. Soc.* **55**, 451–469 (1978).
- Dawson, B. & Smith, M. Veined and metasomatised peridotites from Pello Hill, Tanzania: evidence for anomalously light mantle beneath the Tanzania sector of the eastern rift valley. *Contrib. Mineral. Petrol.* **100**, 510–527 (1988).
- Bosworth, W. & Morley, C. K. Structural and stratigraphic evolution of the Anza rift, Kenya. *Tectonophysics* **236**, 93–115 (1994).
- Coffin, M. F., Rabinowitz, P. & Houtz, R. E. Crustal structure in the western Somali basin. *Geophys. J. R. Astron. Soc.* **86**, 331–365 (1986).
- Richards, M., Duncan, R. & Courtillot, V. Flood basalts and hotspot tracks: plume heads and tails. *Science* **246**, 103–107 (1989).
- van der Meer, F. & Cloetingh, S. Intraplate stresses and the subsidence history of the Sirte basin (Libya). *Tectonophysics* **226**, 37–58 (1993).
- Coffin, M. & Rabinowitz, P. *Evolution of the Conjugate Madagascar and W. Somali Basin* (Spec. Publ. 226, Geol. Soc. Am., Boulder, Colorado, (1988).
- Huppert, H. E. The propagation of two-dimensional axisymmetric viscous gravity currents over a rigid horizontal surface. *J. Fluid Mech.* **121**, 43–58 (1982).

Acknowledgements. C.J.E. completed this work while on sabbatical leave at Stanford University. We thank G. Davies for detailed comments, and M. Menzies, G. Thompson, K. Burke, C. Ruppel, T. Parsons, R. George, G. Barth and J. Cann for discussions, which improved this work.

Correspondence and requests for materials should be addressed to C.J.E. at the University of Leeds (e-mail: cindy@earth.leeds.ac.uk).